

SURFACE CROUZEIX-RAVIART ELEMENT FOR THE LAPLACE-BELTRAMI EQUATION

HAILONG GUO*

Abstract. This paper is concerned with the nonconforming finite element discretization of geometric partial differential equations. In specific, we construct a surface Crouzeix-Raviart element on the linear approximated surface, analogous to a flat surface. The optimal error estimations are established even though the presentation of the geometric error. By taking the intrinsic viewpoint of manifolds, we introduce a new superconvergent gradient recovery method for the surface Crouzeix-Raviart element using only the information of discretization surface. The potential of serving as an asymptotically exact *a posteriori* error estimator is also exploited. A series of benchmark numerical examples are presented to validate the theoretical results and numerically demonstrate the superconvergence of the gradient recovery method.

AMS subject classifications. Primary 65N30; Secondary 45N08

Key words. Laplace-Beltrami operator, nonconforming, surface finite element method, Crouzeix-Raviart element, gradient recovery, superconvergence.

1. Introduction. Numerical methods for approximating partial differential equations (PDEs) with solutions defined on surfaces are of growing interests over the last decades. Since the pioneer work of Dziuk [25], there is tremendous development on finite element methods [2, 13, 17, 20–22, 26, 29, 31, 35, 36]. Fluid equations on manifolds have many important applications in fluidic biomembranes [3, 6], computer graphics [27, 33], geophysics [37, 41]. Typically, numerical simulation of surface Stokes or Navier-Stokes equations is unavoidable. In the literature, there are several works on them, for example, see [7, 28, 34, 38, 39]. It is well known that linear surface element is not a stable pair for surface Stokes equations [12]. One can fix it by adding a stabilizing term [34, 39] or using Taylor-Hood element [28].

In the planar domain case, a simpler way to overcome this difficulty is to use the Crouzeix-Raviart element. The Crouzeix-Raviart element was firstly proposed by Crouzeix and Raviart in [18] to solve a steady Stokes equation. Different from the Courant element, such element is only continuous at edge centers of a triangulation. In that sense, it is a nonconforming element. In addition to being used to construct a simple stable finite element pair for Stoke problems, the method is also proven to be locking free for Lamé problems [11]. It can be viewed as a universal element for solids, fluids, and electromagnetic, see the recent review paper [9] and the references therein.

Our first purpose is to extend this exotic nonconforming element to a surface setting. Compared with the counterpart in the flat space, there is an additional geometric error due to the discretization of the surface. One of the main difficulties is to estimate the nonconforming error. The key ingredient of this step is to conduct all the error analysis on the discretized surface instead of on the exact surface. It should be pointed out that, in general, two triangles sharing a common edge are not on the same plane. The standard argument [8, 16] for nonconforming finite element method cannot be applied directly and the nonconforming error is coupled together with the

*School of Mathematics and Statistics, The University of Melbourne, Parkville, VIC 3010, Australia (hailong.guo@unimelb.edu.au). This work was partially supported by Andrew Sisson Fund of the University of Melbourne.

geometric error. By carefully using the geometric approximation properties, we show that the geometric error has no impact on the overall convergence results.

Our second purpose is to propose a superconvergent post-processing technique for the surface Crouzeix-Raviart element. On the planar domain case, there are several post-processing techniques [14, 30] for the Crouzeix-Raviart element. In particular, Guo and Zhang employed a local least-squares fitting procedure at every edge center to generate a more accurate approximate gradient. The most straightforward way of generalizing such idea to a surface setting is to project a local patch onto its tangent plane as in [42]. However, there are two barriers to the surface Crouzeix-Raviart element: first, it requires the exact normal vectors; second, it requires the edge centers located on the exact surface. Those two difficulties can be alleviated by going back to the original definition of the covariant derivative as in [24]. In specific, we firstly adopt a least-squares procedure to recover the local parametric map and then employ another least-squares fitting on the parameter domain. Based on the gradient recovery method, we introduce a recovery-type *a posteriori* error estimator for the surface Crouzeix-Raviart element.

The rest of the paper is organized as the follows. In section 2, we give a brief introduction to some preliminary knowledge on the tangential derivative and an exemplary model problem. In section 3, we introduce the discretized surface and present the surface Crouzeix-Raviart element. Section 4 is devoted to the analysis of discrete energy error and L^2 error on the discrete surface. In section 5, we propose a superconvergent post-processing technique. A series of benchmark numerical examples are presented to support our theoretical finding in Section 6. Some conclusions are drawn in Section 7.

2. Preliminary.

2.1. Notation. In the paper, we shall consider Γ is an oriented, connected, C^∞ smooth regular surface in \mathbb{R}^3 without boundary. The sign distance function of Γ is denoted by $d(x)$. Let ∇ be the standard gradient operator in \mathbb{R}^3 . Then the unit outward-pointing normal vector is $n(x) = \nabla d(x)$ and the Weingarten map is $\mathbf{H}(x) = \nabla n(x) = \nabla^2 d(x)$.

Let $U = \{x \in \mathbb{R}^3 : \text{dist}(x, \Gamma) \leq \delta\}$ be a strip neighborhood around Γ with distance δ where $\text{dist}(x, \Gamma)$ is the Euclidean distance between x and Γ . Assume δ is small enough such that there exists a unique projection $p(x) : U \rightarrow \Gamma$ in the form of

$$p(x) = x - d(x)n(p(x)). \quad (2.1)$$

Let $P = Id - n \otimes n$ be the tangential projection operator where \otimes is the tensor product. The tangential gradient of a scalar function v on Γ is defined to be

$$\nabla_\Gamma u = P\nabla u = \nabla u - (\nabla u \cdot n)n. \quad (2.2)$$

For a vector field $w \in \mathbb{R}^3$, the tangential divergence is

$$\text{div}_\Gamma w = \nabla_\Gamma \cdot w = \nabla \cdot w - n^t \nabla w n \quad (2.3)$$

The Laplace-Beltrami operator Δ_Γ is just the tangential divergence of the tangential gradient, i.e.

$$\Delta_\Gamma v = \text{div}_\Gamma \nabla_\Gamma v = \Delta v - (\nabla v \cdot n)(\nabla \cdot n) - n^t \nabla^2 v n. \quad (2.4)$$

Let $\alpha = (\alpha_1, \alpha_2, \alpha_3)$ be the 3-index and $|\alpha| = \sum_{i=1}^3 \alpha_i$ with α_i being a nonnegative integer. Let D_Γ^α be the $|\alpha|$ th order tangential derivative. Assume ω being a subset of

Γ and m being a nonnegative integer. The Sobolev space $H^m(\omega)$ on ω [43] is defined as

$$H^m(\omega) = \{v \in L^2(\omega) | D_\Gamma^\alpha v \in L^2(\omega), |\alpha| \leq m\}, \quad (2.5)$$

with norm

$$\|v\|_{H^m(\omega)} = \left(\sum_{\alpha \leq m} \|D_\Gamma^\alpha v\|_{L^2(\omega)}^2 \right)^{1/2}, \quad (2.6)$$

and semi-norm

$$|v|_{H^m(\omega)} = \left(\sum_{\alpha=m} \|D_\Gamma^\alpha v\|_{L^2(\omega)}^2 \right)^{1/2}. \quad (2.7)$$

Throughout this article, we use $x \lesssim y$ to denote $x \leq Cy$ where the letter C denotes a generic constant which is independent of h and may not be the same at each occurrence.

2.2. Model problem. In this paper, we shall consider the following model Laplace-Beltrami equation

$$-\Delta_\Gamma u + u = f, \quad (2.8)$$

for a given $f \in L^2(\Gamma)$.

The variational formulation of (2.8) is to find $u \in H^1(\Gamma)$ such that

$$a(u, v) = \ell(v), \quad \forall v \in H^1(\Gamma) \quad (2.9)$$

where

$$a(w, v) = (\nabla_\Gamma w, \nabla_\Gamma v) + (w, v), \quad (2.10)$$

and

$$\ell(v) = (f, v), \quad (2.11)$$

with (\cdot, \cdot) being the standard L^2 inner product on Γ . The Lax-Milligram theorem implies (2.9) has a unique solution and there holds the following regularity [4]

$$\|u\|_{H^2(\Gamma)} \lesssim \|f\|_{L^2(\Gamma)}. \quad (2.12)$$

3. The nonconforming finite element method.

3.1. Approximate surface. Suppose Γ_h is a polyhedral approximation of Γ with planar triangular surface. Let \mathcal{T}_h be the associated mesh of Γ_h and $h = \max_{T \in \mathcal{T}_h} \text{diam}(T)$ be its maximum diameter. Furthermore, we assume the mesh \mathcal{T}_h is sharp regular and quasi-uniform triangulation [8, 10, 16] and all vertices lie on Γ . Let \mathcal{E}_h be the set of all edges of triangular faces in \mathcal{T}_h . For any edge $E \in \mathcal{E}_h$, let m_E be the middle point of edge E . The set of all edge middle points of \mathcal{T}_h is denoted by \mathcal{M}_h . For any $T \in \mathcal{T}_h$, let n_h be the unit outer normal vector to Γ_h on T . The projection onto the tangent space of Γ_h can be defined

$$P_h = Id - n_h \otimes n_h. \quad (3.1)$$

Similarly, for a scalar function v on Γ_h , we can define its tangential gradient as

$$\nabla_{\Gamma_h} v = P_h \nabla v, \quad (3.2)$$

and the Laplace-Beltrami operator on Γ_h as

$$\Delta_{\Gamma_h} v = \nabla_{\Gamma_h} \cdot \nabla_{\Gamma_h} v_h \quad (3.3)$$

Recall that $p(x)$ is a projection map from U to Γ . For any $T \in \mathcal{T}_h$, let $T^l = p(T)$ be the curved triangular face on Γ . Denote the set of all curved triangular faces by \mathcal{T}_h^l , i.e. $\mathcal{T}_h^l = \{T^l : T \in \mathcal{T}_h\}$. Then \mathcal{T}_h^l forms a conforming triangulation of Γ such that

$$\Gamma = \bigcup_{T^l \in \mathcal{T}_h^l} T^l. \quad (3.4)$$

For any edge $E \in \mathcal{E}_h$, there exists two triangles T^+ and T^- such that $E = \partial T^+ \cap \partial T^-$. The projection on T^+ and T^- are denoted by P_h^+ and P_h^- . Also, we use the notation $\nabla_{\Gamma_h}^+ = P_h^+ \nabla$ to denote the tangent gradient in T^+ . Similar notation is adopted in T^- . The conormal of E to T^+ , which is denoted by n_E^+ , is the unit outward vector of E in the tangent plane of T^+ . Similarly, let n_E^- be the conormal of E to T^- . Analogously, on the curved edge $E^l = p(E)$, we denote its conormals by $n_{E^l}^\pm$. Note that $n_{E^l}^+ = -n_{E^l}^-$. The unit outer normals of Γ_h on T^+ and T^- are denoted by n_h^+ and n_h^- , respectively. Then it easy see that $n_h^+ \perp n_E^+$ and $n_h^- \perp n_E^-$. We define the jump of a function v_h across E by

$$[[v]] = \lim_{s \rightarrow 0_+} (v(x - sn_E^+) - v(x - sn_E^-)). \quad (3.5)$$

3.2. The surface Crouzeix-Raviart finite element method. The surface Crouzeix-Raviart finite element space on \mathcal{T}_h is defined to be

$$V_h = \{v_h \in L^2(\Gamma_h) : v_h|_T \in \mathbb{P}^1(T) \text{ and } v_h \text{ is continuous at } \mathcal{M}_h\}, \quad (3.6)$$

where $\mathbb{P}_1(T)$ is the set of linear polynomials on T . By the definition of jump (3.5) and the midpoint rule, a piecewise linear function v is in V_h if and only if

$$\int_E [[v]] d\sigma_h = 0. \quad (3.7)$$

To simplify the notation, we firstly define a discrete bilinear form $a_h(\cdot, \cdot)$ on $V_h \times V_h$ as

$$a_h(w_v, v_h) = \sum_{T \in \mathcal{T}_h} \int_T \nabla_{\Gamma_h} w_h \cdot \nabla_{\Gamma_h} v_h \cdot ds_h + (w_h, v_h)_{\Gamma_h} \quad (3.8)$$

and a linear functional $\ell_h(\cdot)$ on V_h as

$$\ell_h(v_h) = (f \circ p, v_h)_{\Gamma_h} \quad (3.9)$$

where $(\cdot, \cdot)_{\Gamma_h}$ is the standard L^2 inner product of $L^2(\Gamma_h)$. Then the surface Crouzeix-Raviart finite element discretization of the model problem (2.8) reads as: find $u_h \in V_h$ such that

$$a_h(u_h, v_h) = \ell_h(v_h), \quad \forall v_h \in V_h. \quad (3.10)$$

We define an broken H_1 semi-norm on V_h as

$$|v_h|_{H^1(\Gamma_h; \mathcal{T}_h)}^2 = \sum_{T \in \mathcal{T}_h} \|\nabla_{\Gamma_h} v_h\|_{L^2(T)}^2 \quad (3.11)$$

The corresponding discrete energy norm is given by

$$\|v\|_h^2 = |v_h|_{H^1(\Gamma_h; \mathcal{T}_h)}^2 + \|v_h\|_{L^2(\Gamma_h)}^2 = a_h(v_h, v_h). \quad (3.12)$$

Then, it is easy to show that following Lemma:

LEMMA 3.1. $\|v\|_h$ is a norm on V_h . The Lax-Milgram theorem implies the discrete variational problem (3.10) admits a unique solution.

4. A priori error estimates.

4.1. Lift and extension functions. To compare the error between the exact solution u defined on Γ and the finite element solution u_h defined on Γ_h , we need to establish connections between the functions defined on Γ and Γ_h .

Following the notation as in [13], for a function v defined on Γ , we extend it to U and define the extension v^e by

$$v^e(x) = v(p(x)), \quad \forall x \in U. \quad (4.1)$$

Similarly, for a function v_h defined on Γ_h , we define the lift of v_h onto Γ by

$$v^l(x) = v(\xi(x)), \quad \forall x \in \Gamma, \quad (4.2)$$

where $\xi(x)$ is the unique solution of

$$x = p(\xi) = \xi - d(\xi)n(x). \quad (4.3)$$

Then we build the relationship in gradients of extensions and lifts. For such propose, we introduce the matrix $B = P(x) - d(x)H(x)$. It is easy to check that $B = PB = BP = PBP$. The following relationship is proved in [13, 22, 31]

$$\nabla_{\Gamma_h} v^e = P_h B (\nabla_{\Gamma} v)^e. \quad (4.4)$$

Let ds and ds_h be the surface measures of Γ and Γ_h . For any $x \in \Gamma_h$, [22] shows that there exists μ_h such that $ds \circ p(x) = \mu_h(x) ds_h(x)$ with

$$\mu_h(x) = (1 - d(x)k_1(x))(1 - d(x)k_2(x))n \cdot n_h. \quad (4.5)$$

Throughout the paper, we assume that $\Gamma_h \subset U$. In the following, we collect some geometric approximation results which will be used in our proof:

LEMMA 4.1. Suppose $\Gamma_h \subset U$ is a polyhedral approximation of Γ . Assume the mesh size h is small enough. Then the following error estimates hold:

$$\|d\|_{L^\infty(T)} \lesssim h^2, \quad (4.6)$$

$$\|1 - \mu_h\|_{L^\infty(T)} \lesssim h^2, \quad (4.7)$$

$$\|n - n_h\|_{L^\infty(T)} \lesssim h, \quad (4.8)$$

$$\|P - P_h\|_{L^\infty(T)} \lesssim h, \quad (4.9)$$

$$\|n_{E^l}^{+/-} - Pn_E^{+/-}\|_{L^\infty(T)} \lesssim h^2, \quad (4.10)$$

$$\|\Delta_{\Gamma_h} u^e - (\Delta_{\Gamma} u)^e\|_{L^2(T)} \lesssim h \|u\|_{H^2(T^l)}, \quad (4.11)$$

where $|\cdot|$ is the standard Euclidean norm.

Proof. The inequalities (4.6)–(4.9) can be proved using the standard linear interpolation theory. Their proof can be found in [22]. The last two estimates were proved in [31]. \square

REMARK 4.1. For the planar domain case, it is well known that $n_E^+ = -n_E^-$ and hence $|n_E^+ + n_E^-| = 0$. But this relationship does not hold any more in the surface setting.

To connect the function defined on the exact surface and its extension on the discrete surface, we need the following norm equivalence theorem whose proof can be proved in [25, 31]

LEMMA 4.2. Let $T \in \mathcal{T}_h$. If $v \in H^2(T)$, then the following results hold:

$$\|v^l\|_{L^2(T^l)} \lesssim \|v\|_{L^2(T)} \lesssim \|v^l\|_{L^2(T^l)}, \quad (4.12)$$

$$|v^l|_{H^1(T^l)} \lesssim |v|_{H^1(T)} \lesssim |v^l|_{H^1(T^l)}, \quad (4.13)$$

$$|v|_{H^2(T)} \lesssim \|v^l\|_{H^2(T^l)}, \quad (4.14)$$

$$|v^l|_{H^2(T^l)} \lesssim \|v\|_{H^2(T)}. \quad (4.15)$$

Also, we need the following norm equivalence results for function defined on the edge of an element [13]

LEMMA 4.3. Let $E \in \mathcal{E}_h$. If $v \in H^1(E)$, then the following results hold:

$$\|v^l\|_{L^2(E^l)} \lesssim \|v\|_{L^2(E)} \lesssim \|v^l\|_{L^2(E^l)}, \quad (4.16)$$

$$|v^l|_{H^1(E^l)} \lesssim |v|_{H^1(E)} \lesssim |v^l|_{H^1(E^l)}. \quad (4.17)$$

4.2. The nonconforming interpolation. For any $T \in \mathcal{T}_h$, let \mathcal{E}_T be the set of three edges of T . We define the local interpolation operator $\Pi_T : H^1(T) \rightarrow \mathbb{P}_1(T)$ by

$$(\Pi_T v)(m_E) = \frac{1}{|E|} \int_E v d\sigma_h, \quad \forall v \in H^1(T), E \in \mathcal{E}_T, \quad (4.18)$$

where $|E|$ is the length of E . By the midpoint rule, we can show that

$$\int_E (\Pi_T v) d\sigma_h = \int_E v d\sigma_h, \quad E \in \mathcal{E}_T. \quad (4.19)$$

Let h_T be the diameter of T . Then the following error estimate holds [9, 18]

$$\|v - \Pi v\|_{L^2(T)} + h_T |v - \Pi v|_{H^1(T)} \lesssim h_T^2 |v|_{H^2(T)}, \quad (4.20)$$

for any $v \in H^2(T)$. The global interpolation operator $\Pi_h : H^1(\Gamma_h) \rightarrow V_h$ is defined by

$$(\Pi_h v)|_T = \Pi_T v, \quad \forall T \in \mathcal{T}_h. \quad (4.21)$$

It follows from (4.20) that

$$\|v - \Pi_h v\|_{L^2(\Gamma_h)} + h |v - \Pi_h v|_{H^1(\Gamma_h; \mathcal{T}_h)} \lesssim h^2 |v|_{H^2(\Gamma_h)}, \quad (4.22)$$

In particular, let $v = u^e$. Then we have

$$\inf_{v_h \in V_h} \|u^e - v_h\|_h \leq |v - \Pi_h v|_{H^1(\Gamma_h; \mathcal{T}_h)} + \|u - \Pi_h u^e\|_{L^2(\Gamma_h)} \lesssim h |u^e|_{H^2(\Gamma_h)}. \quad (4.23)$$

4.3. Energy error estimate. In this subsection, we establish the error bound in the discrete energy error. Our main tool of the error estimation is the second Strang Lemma [8, 10, 16]:

LEMMA 4.4 (The second Strang Lemma). *Suppose u is the exact solution of (2.9) and u_h is the finite element solution of (3.10). Then we obtain that*

$$\|u^e - u_h\|_h \lesssim \inf_{v_h \in V_h} \|u^e - v_h\|_h + \sup_{w_h \in V_h} \frac{|a_h(u^e, w_h) - (f^e, w_h)|}{\|w_h\|_h} \quad (4.24)$$

REMARK 4.2. *We also call the first term is the approximation error and the second term is the nonconforming consistency error. But different from the planar domain case, the second term also involves the geometric error in addition to the classical nonconforming consistency error. We measure the error using the discrete energy norm on the approximate surface and this is the key part to bound the nonconforming consistency error.*

We prepare the energy error estimation with some geometric error estimates. We begin with the following Lemma:

LEMMA 4.5. *Let u be the solution of (2.9) and u^e be its extension to U defined by (4.1). Then we have the following error estimates holds*

$$|(u, w_h^l) - (u^e, w_h)_{\Gamma_h}| \lesssim h^2 \|u\|_{L^2(\Gamma)} \|w_h\|_{L^2(\Gamma_h)}, \quad (4.25)$$

$$|(f, w_h^l) - (f^e, w_h)_{\Gamma_h}| \lesssim h^2 \|f\|_{L^2(\Gamma)} \|w_h\|_{L^2(\Gamma_h)}. \quad (4.26)$$

for any $w_h \in V_h$.

Proof. We only prove (4.26) and (4.25) can be proved similarly. Applying the change of variable, we have

$$|(f, w_h^l) - (f^e, w_h)_{\Gamma_h}| \lesssim |((\mu_h - 1)f^e, w_h)_{\Gamma_h}| \lesssim h^2 \|f^e\|_{L^2(\Gamma_h)} \|w_h\|_{L^2(\Gamma_h)}$$

where we have used the error estimate (4.7). \square

Next, we prove a lemma for estimate the error involving two conomorphals of an edge.

LEMMA 4.6. *Let u be the solution of (2.9) and u^e be its extension to U defined by (4.1). Then we have the following error estimates holds*

$$\sum_{E \in \mathcal{E}_h} \int_E (n_E^+ \cdot \nabla_{\Gamma_h}^+ u^e + n_E^- \cdot \nabla_{\Gamma_h}^- u^e)^2 d\sigma_h \leq h^3 \|u\|_{H^2(\Gamma)}^2. \quad (4.27)$$

Proof. Using the triangle inequality and (4.4), we have

$$\begin{aligned}
& \int_E (n_E^+ \cdot \nabla_{\Gamma_h}^+ u^e + n_E^- \cdot \nabla_{\Gamma_h}^- u^e)^2 d\sigma_h \\
&= \int_E (n_E^+ \cdot P_h^+ B(\nabla_{\Gamma} u)^e + n_E^- \cdot P_h^- B(\nabla_{\Gamma} u)^e)^2 d\sigma_h \\
&= \int_E (Pn_E^+ \cdot B(\nabla_{\Gamma} u)^e + Pn_E^- \cdot B(\nabla_{\Gamma} u)^e)^2 d\sigma_h \\
&\lesssim \int_E ((Pn_E^+ - n_{E^l}^+) \cdot B(\nabla_{\Gamma} u)^e)^2 d\sigma_h + \\
&\quad \int_E ((n_{E^l}^- - Pn_E^-) \cdot B(\nabla_{\Gamma} u)^e)^2 d\sigma_h \\
&\lesssim h^4 \int_E |(\nabla_{\Gamma} u)^e|^2 d\sigma_h \\
&\lesssim h^4 \int_{E^l} |\nabla_{\Gamma} u|^2 d\sigma,
\end{aligned} \tag{4.28}$$

where we have used (4.10) in the second inequality and norm equivalence (4.17) in the last inequality.

Summing over over all $E \in \mathcal{E}_h$ and applying the trace inequality, we have

$$\begin{aligned}
& \sum_{E \in \mathcal{E}_h} \int_E (n_E^+ \cdot \nabla_{\Gamma_h}^+ u^e + n_E^- \cdot \nabla_{\Gamma_h}^- u^e)^2 d\sigma_h \\
&\lesssim h^4 \sum_{E \in \mathcal{E}_h} \int_{E^l} |\nabla_{\Gamma} u|^2 d\sigma \\
&\lesssim h^4 \sum_{T \in \mathcal{T}_h} \int_{\partial T^l} |\nabla_{\Gamma} u|^2 d\sigma \\
&\lesssim h^4 \sum_{T \in \mathcal{T}_h} \left(h^{-1} \|\nabla u\|_{L^2(T^l)}^2 + h \|\nabla u\|_{H^1(T^l)}^2 \right) \\
&\lesssim h^3 \|u\|_{H^2(\Gamma)}^2,
\end{aligned} \tag{4.29}$$

which completes our proof. \square

In the next Lemma, we estimate the main term in the nonconforming consistency error by using an argument analogous to the Crouzeix-Raviart element in planar domain [8].

LEMMA 4.7. *Let u be the solution of (2.9) and u^e be its extension to U defined by (4.1). Then we have the following error estimates holds*

$$\sum_{E \in \mathcal{E}_h} \int_E n_E^+ \cdot \nabla_{\Gamma_h}^+ u^e \llbracket w_h \rrbracket d\sigma_h \lesssim h |u^e|_{H^2(\Gamma)} |w_h|_{H^1(\Gamma_h; \mathcal{T}_h)}. \tag{4.30}$$

for any $w_h \in V_h$.

Proof. Let $\Pi_E^0 w_h = \frac{1}{|E|} \int_E w_h d\sigma_h$. Using the fact $\llbracket \Pi_E^0 w_h \rrbracket = 0$ and the Cauchy

Schwartz inequality, we have

$$\begin{aligned}
& \sum_{E \in \mathcal{E}_h} \int_E n_E^+ \cdot \nabla_{\Gamma_h}^+ u^e \llbracket w_h \rrbracket d\sigma_h \\
&= \sum_{E \in \mathcal{E}_h} \int_E n_E^+ \cdot \nabla_{\Gamma_h}^+ u^e \llbracket w_h - \Pi_E^0 w_h \rrbracket d\sigma_h \\
&= \sum_{E \in \mathcal{E}_h} \int_E n_E^+ \cdot \nabla_{\Gamma_h}^+ (u^e - \Pi_h u^e) \llbracket w_h - \Pi_E^0 w_h \rrbracket d\sigma_h \\
&= \sum_{E \in \mathcal{E}_h} \left(\int_E |\nabla_{\Gamma_h}^+ (u^e - \Pi_h u^e)|^2 d\sigma_h \right)^{1/2} \left(\int_E \llbracket w_h - \Pi_E^0 w_h \rrbracket^2 d\sigma_h \right)^{1/2}
\end{aligned} \tag{4.31}$$

Arguing similarly using the trace inequality, the Poincaré's inequality and (4.20) as in planar domain [8], we obtain

$$\int_E |\nabla_{\Gamma_h}^+ (u^e - \Pi_h u^e)|^2 d\sigma_h \lesssim h |u|_{H^2(T^+)}, \tag{4.32}$$

$$\int_E \llbracket w_h - \Pi_E^0 w_h \rrbracket^2 d\sigma_h \lesssim h \left(|w_h|_{H^1(T^+)}^2 + |w_h|_{H^1(T^-)}^2 \right). \tag{4.33}$$

Combing the estimates (4.31)–(4.33) gives (4.30). \square

Now, we are prepared to prove the nonconforming consistency error:

LEMMA 4.8. *Let u be the solution of (2.9) and u^e be its extension to U defined by (4.1). Then we have the following error estimates holds*

$$|a_h(u^e, w_h) - (f^e, w_h)_{\Gamma_h}| \lesssim h \|u\|_{H^2(\Gamma)} \|w_h\|_h. \tag{4.34}$$

for any $w_h \in V_h$.

Proof. For any $w_h \in V_h$, we notice that

$$a_h(u^e, w_h) - (f^e, w_h)_{\Gamma_h} = [a_h(u^e, w_h) - (f, w_h^l)] + [(f, w_h^l) - (f^e, w_h)_{\Gamma_h}]. \tag{4.35}$$

Using (4.26), the second term can be estimated as

$$|(f, w_h^l) - (f^e, w_h)_{\Gamma_h}| \lesssim h^2 \|f\|_{L^2(\Gamma)} \|w_h\|_{L^2(\Gamma_h)} \lesssim h^2 \|u\|_{H^2(\Gamma)} \|w_h\|_h. \tag{4.36}$$

where we used the fact $f = -\Delta_{\Gamma} u + u$.

To estimate the first term, we apply the Green's formula and we obtain that

$$\begin{aligned}
& a_h(u^e, w_h) - (f, w_h^l) \\
&= \sum_{E \in \mathcal{E}_h} \int_E (n_E^+ \cdot \nabla_{\Gamma_h}^+ u^e w_h^+ + n_E^- \cdot \nabla_{\Gamma_h}^- u^e w_h^-) d\sigma_h - \\
& \quad \sum_{T \in \mathcal{T}_h} (\Delta_{\Gamma_h} u^e, w_h)_T + (\Delta_{\Gamma} u, w_h^l) + (u^e, w_h)_{\Gamma_h} - (u, w_h^l) \\
&= \sum_{E \in \mathcal{E}_h} \int_E (n_E^+ \cdot \nabla_{\Gamma_h}^+ u^e + n_E^- \cdot \nabla_{\Gamma_h}^- u^e) w_h^- d\sigma_h + [(u^e, w_h)_{\Gamma_h} - (u, w_h^l)] \\
& \quad \sum_{E \in \mathcal{E}_h} \int_E n_E^+ \cdot \nabla_{\Gamma_h}^+ u^e \llbracket w_h \rrbracket d\sigma_h + \left[(\Delta_{\Gamma} u, w_h^l) - \sum_{T \in \mathcal{T}_h} (\Delta_{\Gamma_h} u^e, w_h)_T \right] \\
&= I_1 + I_2 + I_3 + I_4.
\end{aligned} \tag{4.37}$$

To estimate I_1 , we use Lemma 4.6, the Cauchy-Schwartz inequality, and the trace inequality to get

$$\begin{aligned} |I_1| &\leq \left(\sum_{E \in \mathcal{E}_h} \int_E (n_E^+ \cdot \nabla_{\Gamma_h}^+ u^e + n_E^- \cdot \nabla_{\Gamma_h}^- u^e)^2 d\sigma_h \right)^{1/2} \left(\sum_{E \in \mathcal{E}_h} \int_E (w_h^-)^2 d\sigma_h \right)^{1/2} \\ &\lesssim h^{3/2} \|u\|_{H^2(\Gamma)} \left(h^{-1/2} \|w_h\|_{L^2(\Gamma_h)} + h^{1/2} |w_h|_{H^1(\Gamma_h; \mathcal{T}_h)} \right) \\ &\lesssim h \|u\|_{H^2(\Gamma)} \|w_h\|_h. \end{aligned}$$

According to Lemma 4.5 and Lemma 4.6, we have

$$|I_2| + |I_3| \lesssim h \|u\|_{H^2(\Gamma)} \|w_h\|_h.$$

Then, we estimate I_4 . By the triangle inequality and the error estimate (4.11) and (4.9), we have

$$\begin{aligned} |I_4| &= \left| \sum_{T \in \mathcal{T}} (\Delta_{\Gamma} u, w_h^l)_{T^l} - \sum_{T \in \mathcal{T}_h} (\Delta_{\Gamma_h} u^e, w_h)_{T^l} \right| \\ &\leq \sum_{T \in \mathcal{T}} |(\mu_h (\Delta_{\Gamma} u)^e, w_h^l)_{T^l} - (\Delta_{\Gamma_h} u^e, w_h)_{T^l}| \\ &\leq \sum_{T \in \mathcal{T}} |((\mu_h - 1) (\Delta_{\Gamma} u)^e, w_h)_{T^l}| + \sum_{T \in \mathcal{T}} |((\Delta_{\Gamma} u)^e - \Delta_{\Gamma_h} u^e, w_h)_{T^l}| \\ &\lesssim h \|u\|_{H^2(\Gamma)} \|w_h\|_{L^2(\Gamma_h)}. \end{aligned}$$

Summing the above three error estimates, we complete the proof of (4.34). \square

With all the previous preparations, we are in perfect position to prove the following energy error estimate

THEOREM 4.9. *Let u be the solution of (2.9) and u^e be its extension to U defined by (4.1). Then we have the following error estimates holds*

$$\|u^e - u_h\|_h \lesssim h \|f\|_{L^2(\Gamma)}. \quad (4.38)$$

Proof. Using Lemma 4.8 and the regularity estimate (2.12), we obtain that

$$\sup_{w_h \in V_h} \frac{|a_h(u^e, w_h) - \ell(w_h^l)|}{\|w_h\|_h} \lesssim h \|f\|_{L^2(\Gamma)}. \quad (4.39)$$

We complete our proof by combining the Strang Lemma 4.4 and the estimates (4.23) and (4.39). \square

4.4. L_2 error estimate. In this subsection, we establish a priori error estimate in L^2 norm using the Abuin-Nitsche's trick [8, 10, 16]. Let $g = u - u_h^l \in L^2(\Gamma)$. The dual problem is to find $\phi \in H^1(\Gamma)$ such that

$$a(v, \phi) = (v, g), \quad \forall v \in H^1(\Gamma). \quad (4.40)$$

Similarly, we have the following regularity result:

$$\|\phi\|_{H^2(\Gamma)} \leq \|g\|_{L^2(\Gamma)}. \quad (4.41)$$

The surface Crouzeix-Raviart element discretization of the dual problem is to find $\phi_h \in V_h$ such that

$$a_h(v_h, \phi_h) = (v_h, g^e), \quad \forall v_h \in V_h, \quad (4.42)$$

where $g^e = (u - u_h^l)^e = u^e - u_h$. By Theorem 4.9, we have the following energy error estimate

$$\|\phi^e - \phi_h\|_h \lesssim h \|g\|_{L^2(\Gamma)}. \quad (4.43)$$

We begin our L^2 error estimate with the following Lemma:

LEMMA 4.10. *Let u be the solution of (2.9) and ϕ be the solution of the dual problem (4.40). Then we have the following error estimate*

$$a_h(u^e, \phi^e) - a(u, \phi) \lesssim h^2 \|u\|_{H^2(\Gamma)} \|\phi\|_{H^2(\Gamma)}. \quad (4.44)$$

Proof. (4.44) can be proved by using the same technique as in continuous linear surface finite element, see [25]. \square

Then we prove a lemma involving global interpolation Π_h .

LEMMA 4.11. *Let u be the solution of (2.9) and ϕ be the solution of the dual problem (4.40). Then we have the following error estimate*

$$a_h(u^e, \phi^e - \Pi_h \phi^e) \lesssim h^2 \|u\|_{H^2(\Gamma)} \|\phi\|_{H^2(\Gamma)}, \quad (4.45)$$

$$a_h(u^e - \Pi_h u^e, \phi^e) \lesssim h^2 \|u\|_{H^2(\Gamma)} \|\phi\|_{H^2(\Gamma)}. \quad (4.46)$$

Proof. We only give a proof of (4.45) and (4.46) can be proved similarly. To prove (4.45), we apply the integration by part formula and use (4.19) which gives

$$\begin{aligned} a_h(u^e, \phi^e - \Pi_h \phi^e) &= \sum_{T \in \mathcal{T}_h} (\nabla_{\Gamma_h} u^e, \nabla_{\Gamma_h} (\phi^e - \Pi_h \phi^e)) + (u^e, \phi^e - \Pi_h \phi^e) \\ &= -(\Delta_{\Gamma_h} u^e, \phi^e - \Pi_h \phi^e) + (u^e, \phi^e - \Pi_h \phi^e) \end{aligned}$$

Then (4.45) follows by the Cauchy-Schwartz inequality, the interpolation error estimate (4.22) and the norm equivalence. \square

Using the above Lemma, we can prove the following consistency error estimate:

LEMMA 4.12. *Let u be the solution of (2.9) and ϕ be the solution of the dual problem (4.40). Then we have the following error estimate*

$$a_h(u^e, \phi^e - \phi_h) - ((f, \phi) - (f^e, \phi_h)_{\Gamma_h}) \lesssim h^2 \|u\|_{H^2(\Gamma)} \|\phi\|_{H^2(\Gamma)}, \quad (4.47)$$

$$a_h(u^e - u_h, \phi^e) - ((u, g) - (u_h, g^e)_{\Gamma_h}) \lesssim h^2 \|u\|_{H^2(\Gamma)} \|\phi\|_{H^2(\Gamma)}. \quad (4.48)$$

Proof. To prove (4.47), we notice that

$$\begin{aligned} &a_h(u^e, \phi^e - \phi_h) - [(f, \phi) - (f^e, \phi_h)_{\Gamma_h}] \\ &= [a_h(u^e, \Pi_h \phi^e - \phi_h) - (f^e, \Pi_h \phi^e - \phi_h)_{\Gamma_h}] + a_h(u^e, \phi^e - \Pi_h \phi^e) - \\ &\quad [(f, \phi) - (f^e, \phi^e)_{\Gamma_h}] - (f^e, \phi^e - \Pi_h \phi^e)_{\Gamma_h} \\ &= I_1 + I_2 + I_3 + I_4. \end{aligned}$$

We first estimate I_1 . Using Lemma 4.8, we obtain

$$\begin{aligned} |I_1| &\lesssim h \|u\|_{H^2(\Gamma)} \|\Pi_h \phi^e - \phi_h\|_h \\ &\lesssim h \|u\|_{H^2(\Gamma)} (\|\Pi_h \phi^e - \phi^e\|_h + \|\phi^e - \phi_h\|_h) \\ &\lesssim h^2 \|u\|_{H^2(\Gamma)} \|\phi\|_{H^2(\Gamma)}, \end{aligned}$$

According to Lemma 4.11 and Lemma 4.5, we have

$$|I_2| + |I_3| \lesssim h^2 \|f\|_{L^2(\Gamma)} \|g\|_{L^2(\Gamma)}.$$

To estimate I_4 , we use the Cauchy-Schwartz inequality and (4.22) which yields that

$$|I_4| \leq \|f^e\|_{L^2(\Gamma_h)} \|\phi^e - \Pi \phi^e\|_h \lesssim h^2 \|f\|_{L^2(\Gamma)} \|g\|_{L^2(\Gamma)}.$$

Summing all the above error estimates concludes the proof (4.47). The error estimate (4.48) can be proved in the same way. \square

Now, we are ready to present our error estimate in L^2 norm.

THEOREM 4.13. *Let u be the solution of (2.9) and u^e be its extension to U defined by (4.1). Then we have the following error estimates holds*

$$\|u^e - u_h\|_{L^2(\Gamma_h)} \leq h^2 \|f\|_{L^2(\Gamma)}. \quad (4.49)$$

Proof. Using (2.9), (3.10), (4.40) and (4.42), we have

$$\begin{aligned} \|u^e - u_h\|_{L^2(\Gamma_h)}^2 &= (u^e - u_h, g^e)_{\Gamma_h} \\ &= (u^e, g^e)_{\Gamma_h} - (u, g) + (u, g) - (u_h, g^e) \\ &= (u^e, g^e)_{\Gamma_h} - (u, g) + a(u, \phi) - a_h(u_h, \phi_h) \\ &= [(u^e, g^e)_{\Gamma_h} - (u, g)] + [a(u, \phi) - a_h(u^e, \phi^e)] + [a_h(u^e, \phi^e) - a_h(u_h, \phi_h)] \\ &= [(u^e, g^e)_{\Gamma_h} - (u, g)] + [a(u, \phi) - a_h(u^e, \phi^e)] + a_h(u^e - u_h, \phi^e - \phi_h) + \\ &\quad a_h(u_h, \phi^e - \phi_h) + a_h(u^e - u_h, \phi_h) \\ &= [(u^e, g^e)_{\Gamma_h} - (u, g)] - [a(u, \phi) - a_h(u^e, \phi^e)] + a_h(u^e - u_h, \phi^e - \phi_h) - \\ &\quad [a_h(u^e, \phi^e - \phi_h) - ((f, \phi) - (f^e, \phi_h)_{\Gamma_h})] - \\ &\quad [a_h(u^e - u_h, \phi^e) - ((u, g) - (u_h, g^e)_{\Gamma_h})] \\ &= I_1 + I_2 + I_3 + I_4 + I_5. \end{aligned}$$

We first estimate I_1 . By applying the change of variable and (4.7), we have

$$|I_1| = ((1 - \mu_h)u^e, g^e)_{\Gamma_h} \lesssim h^2 \|u\|_{L^2(\Gamma_h)} \|g\|_{L^2(\Gamma_h)} \lesssim h^2 \|f\|_{L^2(\Gamma)} \|g\|_{L^2(\Gamma)}.$$

The estimate of I_2 is provided by Lemma 4.10 which implies

$$|I_2| \lesssim h^2 \|f\|_{L^2(\Gamma)} \|g\|_{L^2(\Gamma)}.$$

To estimate I_3 , we apply the Cauchy-Schwartz inequality which gives

$$|I_3| \lesssim h^2 \|u^e - u_h\|_h \|\phi^e - \phi_h\|_h \lesssim h^2 \|f\|_{L^2(\Gamma)} \|g\|_{L^2(\Gamma)}$$

According to Lemma 4.11 and Lemma 4.5, we have

$$|I_4| + |I_5| \lesssim h^2 \|f\|_{L^2(\Gamma)} \|g\|_{L^2(\Gamma)}.$$

We complete the proof by combining all the above estimates. \square

5. Superconvergent post-processing. In this section, we generalize the parametric polynomial preserving recovery [24] to the surface Crouzeix-Raviart element.

The key idea of parametric polynomial preserving recovery is to take an intrinsic view on a surface. In that sense, a surface can be understood as a union of locally parametrized patches by Euclidean planar domains [23,32]. Let g be the metric tensor of the surface Γ and $\mathbf{r} : \Omega \subset \mathbb{R}^2 \rightarrow S \subset \Gamma$ be a local geometric mapping. Then the tangent gradient operator ∇_Γ can be equivalently defined as

$$(\nabla_\Gamma u) \circ \mathbf{r} = \nabla \bar{u} (g \circ \mathbf{r})^{-1} \partial \mathbf{r}. \quad (5.1)$$

where $\bar{u} = u \circ \mathbf{r}$ is the pull back of the function u to the local planar parameter domain Ω , $\partial \mathbf{r}$ is the Jacobian of \mathbf{r} , and

$$g \circ \mathbf{r} = \partial \mathbf{r} (\partial \mathbf{r})^T. \quad (5.2)$$

Using the relation (5.2), we can rewrite (5.1) as

$$(\nabla_\Gamma u) \circ \mathbf{r} = \nabla \bar{u} (\partial \mathbf{r})^\dagger, \quad (5.3)$$

where $(\partial \mathbf{r})^\dagger$ denotes the Moore-Penrose inverse of $\partial \mathbf{r}$. As proved in [24], the definition of the tangent gradient (5.1) is invariant under different chosen of regular isomorphic parametrization function \mathbf{r} .

Then our goal is to use this intrinsic definition of the tangent gradient to propose a new gradient recovery method for the surface Crouzeix-Raviart element. Different from the linear surface element, the degrees of freedom of the surface Crouzeix-Raviart element are located on the edge midpoints of the approximate surface triangle instead of their vertices. We follow the idea of the gradient recovery method for the Crouzeix-Raviart element in [30] and define the gradient recovery operator $G_h : V_h \rightarrow V_h$. Given a finite element function $u_h \in V_h$, we only need to define $(G_h u_h)(x_i)$ for all $x_i \in \mathcal{M}_h$.

For any $x_i = m_{E_i} \in \mathcal{M}_h$ and $n \in \mathbb{N}$, define the union of elements around x_i in the first n layers as follows

$$L(x_i, n) = \bigcup \{T : T \in \mathcal{T}_h \text{ and } T \cap L(x_i, n-1) \in \mathcal{E}_h\}, \quad (5.4)$$

with $L(x_i, 0) = \{E_i\}$. Let $\Omega_i = L(x_i, n_i)$ with n_i being the smallest integer such that Ω_i satisfies the rank condition (see [44]) in the following sense:

DEFINITION 5.1. *The local element patch is said to satisfy the rank condition i if it admits a unique least-squares fitted polynomial in (5.5) and (5.6).*

To construct the recovered gradient at the given midpoint x_i , we first choose a vector ϕ_3^i to be the normal vector of the local coordinate system. For the sake of simplicity, we choose $\phi_3^i = (n_{E_i}^+ + n_{E_i}^-)/2$. Then we construct a local parameter domain orthogonal to ϕ_3^i . Select x_i as the original of Ω_i and choose (ϕ_1^i, ϕ_2^i) as the normal basis of Ω_i . We project all the midpoints in L_i onto the parameter domain Ω_i and the projections is denoted by ξ_{i_j} , for $j = 0, \dots, n_i$.

Then, we reconstruct the local approximation surface S_i over Ω_i . As in [24], the approximate surface S_i can be approximated by graph of a quadratic function on Ω_i . That is $S_i = \tilde{\mathbf{r}}_{h,i}(\Omega_i) = \cup_{\xi \in \Omega_i} (\xi, s_i(\xi))$, where

$$s_i = \arg \min_{s \in \mathbb{P}_2(\Omega_i)} \sum_{j=1}^{n_i} |s(\xi_{i_j}) - \langle x_{i_j}, \phi_3^i \rangle|^2, \quad (5.5)$$

where $\langle \cdot, \cdot \rangle$ means the Euclidean inner product in \mathbb{R}^3 .

Our next step is to reconstruct a more accurate gradient for $\nabla \bar{u}_h$ on the parameter domain Ω_i . To do this, we use ξ_{i_j} as sampling points and fit a quadratic polynomial $p_i(\xi)$ over Ω_i in the least-squares sense

$$p_i = \arg \min_{p \in \mathbb{P}_2(\Omega_i)} \sum_{j=0}^{n_i} |p(\xi_{i_j}) - u_h(x_{i_j})|^2. \quad (5.6)$$

Calculate the partial derivatives of both the polynomial approximated surface function in (5.5) and the approximated polynomial function of FEM solution in (5.6), then we can approximate the tangent gradient which is given in (5.3) as

$$(G_h u_h)(x_i) = (\partial_1 p_i(0, 0), \partial_2 p_i(0, 0)) \begin{pmatrix} 1 & 0 & \partial_1 s_i(0, 0) \\ 0 & 1 & \partial_2 s_i(0, 0) \end{pmatrix}^\dagger (\phi_1^i, \phi_2^i, \phi_3^i)^T. \quad (5.7)$$

To multiply with the orthonormal basis $(\phi_1^i, \phi_2^i, \phi_3^i)$ is because we have to unify the coordinates from local ones to a global one.

Let $\{\chi_i(x_i)\}_{x_i \in \mathcal{M}_h}$ be the nodal basis functions of the surface Crouzeix-Raviart element. Then recovered gradient on the whole domain is

$$G_h u_h = \sum_{x_i \in \mathcal{M}_h} (G_h u_h)(x_i) \chi_{x_i}(x), \quad \forall x \in \Gamma_h. \quad (5.8)$$

As a direct application of the gradient recovery method, we naturally define a recovery-type *a posteriori* error estimator for the surface Crouzeix-Raviart element. The local *a posteriori* error estimator on each element T is defined as

$$\eta_{h,T} = \|G_h u_h - \nabla_{\Gamma_h} u_h\|_{L^2(T)}, \quad (5.9)$$

and the global error estimator as

$$\eta_h = \left(\sum_{T \in \mathcal{T}_h} \eta_{h,T}^2 \right)^{1/2}. \quad (5.10)$$

6. Numerical Experiments. In this section, we present several numerical examples to validate the theoretical results and test the performance of the recovery-based *a posteriori* error estimator.

To generate an initial mesh on a general surface, we adopt the three-dimensional surface mesh generation module of the Computational Geometry Algorithms Library [40]. Meshes on finer levels are generated by firstly using uniform refinement for the first two numerical examples or the newest bisection [15] refinement for the other two numerical examples and then projecting them on to the surface. In general case, there is no explicit projection map available. We will adopt the first order approximation of projection map as given in [22]. Therefore the vertices of the meshes are not located on the exact manifold but within a distance of $\mathcal{O}(h^2)$ in our test except for the third numerical example.

For the sake of simplifying the notation, we introduce the following notation for errors

$$\begin{aligned} e &:= \|u^e - u_h\|_{L^2(\Gamma_h)}, & De &:= |u^e - u_h|_{H^1(\Gamma_h; \mathcal{T}_h)}, \\ D_i e &:= \|\Pi_h u^e - u_h\|_{H^1(\Gamma_h; \mathcal{T}_h)}, & D_r e &:= \|\nabla u^e - G_h u_h\|_{L^2(\Gamma_h)}. \end{aligned}$$

In the following tables, all convergence rates are listed in term of the degree of freedom(DOF). Noticing $\text{DOF} \approx 1/h^2$ the corresponding convergence rates in term of the mesh size h is double of what we present in the tables.

6.1. Numerical example 1. In this example, we consider the model problem (2.8) on a general surface firstly introduced by Dziuk in [25]. Figure 6.1 show the discretized surface and its initial mesh. The exact solution $u(x) = x_1x_2$ and the right hand side function f can be computed from u .

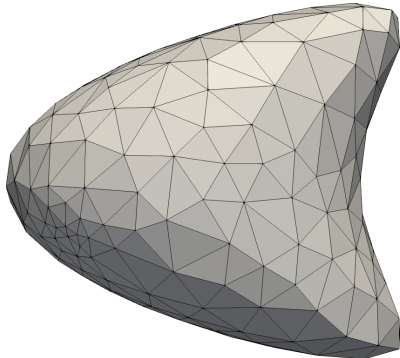


Fig. 6.1: Initial mesh for Dziuk surface

We report the numerical results in Table 6.1. As predict by the Theorem 4.13 and Theorem 4.9, the L_2 error converges at a rate of $\mathcal{O}(h^2)$ and the discrete H^1 semi-error converges at a rate of $\mathcal{O}(h)$. Concerning the error between the finite element gradient and the gradient of the interpolation of the exact solution, $\mathcal{O}(h)$ convergence can be observed. It means that there is no supercloseness between the finite element gradient and the gradient of the interpolation of the exact solution, which is similar to the numerical results in planar domain [30]. Even though in that case, we can observe $\mathcal{O}(h^{1.9})$ superconvergence for the recovered gradient.

Table 6.1: Numerical results for numerical example 1

Dof	e	order	De	order	$D_i e$	Order	$D_r e$	Order
243	3.70e-02	–	6.95e-01	–	2.10e-01	0.00	3.20e-01	–
966	8.51e-03	1.07	3.66e-01	0.46	1.08e-01	0.48	1.07e-01	0.79
3858	2.19e-03	0.98	1.86e-01	0.49	5.49e-02	0.49	3.06e-02	0.90
15426	5.53e-04	0.99	9.37e-02	0.50	2.77e-02	0.50	8.28e-03	0.94
61698	1.39e-04	1.00	4.69e-02	0.50	1.39e-02	0.50	2.23e-03	0.95
246786	3.47e-05	1.00	2.35e-02	0.50	6.93e-03	0.50	6.15e-04	0.93

6.2. Numerical example 2. Our second example to consider a general surface with high curvature part as in [24, 26]. The discretized surface with the initial mesh was plotted in Figure 6.2. We choose f to fit the exact solution $u(x) = x_1x_2$.

In Table 6.2, we list the history of numerical errors. We can observe the same optimal convergence results in L^2 norm and discrete H^1 semi-norm which matches well with the established theoretic results in Section 4. Similar to the previous example, $\mathcal{O}(h^2)$ can be observed even though there is no supercloseness result.

6.3. Numerical example 3. In all the previous numerical examples, the exact solutions are smooth. In this example, we consider a benchmark problem on the unit sphere surface with a singular solution. The solution and the source term in spherical

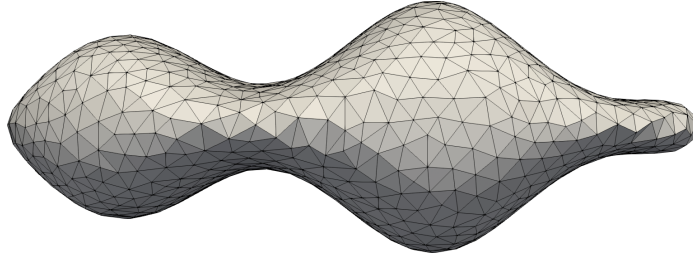


Fig. 6.2: Initial mesh for Elliot surface

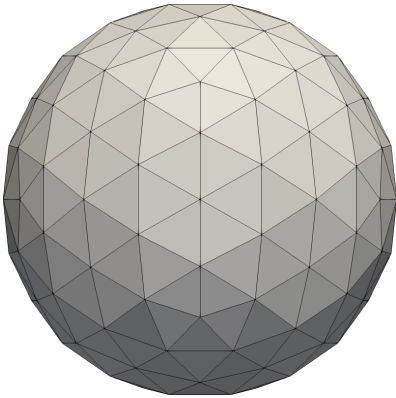
Table 6.2: Numerical results for numerical example 2

Dof	e	order	De	order	$D_i e$	Order	$D_r e$	Order
1153	8.82e+00	–	2.92e+01	–	2.50e+01	–	1.46e+01	–
4606	5.25e-02	3.70	4.24e-01	3.06	2.26e-01	3.40	2.37e-01	2.98
18418	3.92e-03	1.87	1.86e-01	0.60	5.37e-02	1.04	7.19e-02	0.86
73666	1.08e-03	0.93	9.28e-02	0.50	2.65e-02	0.51	1.98e-02	0.93
294658	2.54e-04	1.05	4.64e-02	0.50	1.32e-02	0.50	5.11e-03	0.98
1178626	6.23e-05	1.01	2.32e-02	0.50	6.59e-03	0.50	1.31e-03	0.98

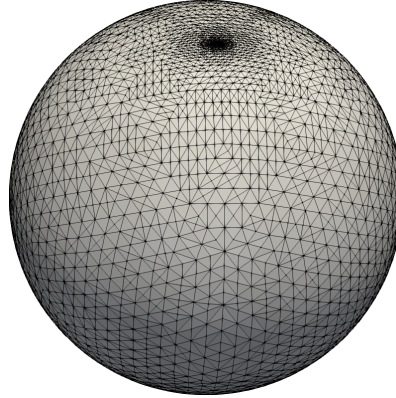
coordinates are given by

$$u = \sin^\lambda(\theta) \sin(\phi), \quad f = (2 + \lambda^2 + \lambda) \sin^\lambda(\theta) \sin(\phi) + (1 - \lambda^2) \sin^{\lambda-2}(\theta) \sin(\phi).$$

It is easy to show that $u \in H^{1+\lambda}(\Gamma)$. When $\lambda < 1$, the solution u has two singularities at north and south poles.



(a)



(b)

Fig. 6.3: Meshes for numerical example 3: (a) Initial mesh; (b) Adaptively refined mesh.

To resolve the singularity, we apply the adaptive finite element method with the recovery based *a posteriori* error estimator (5.9). The initial mesh is icosphere mesh

as plotted in Figure 6.3a. Figure 6.3b plot the adaptive refined meshes after 14 adaptive refinements. It obvious that the refinement is mainly concentrated on the two singular points. We plot the errors in Figure 6.4a. The L^2 error and discrete H^1 semi-error both converges optimally. The recovered gradient superconverges to the exact gradient at a rate of $\mathcal{O}(h^{1.6})$.

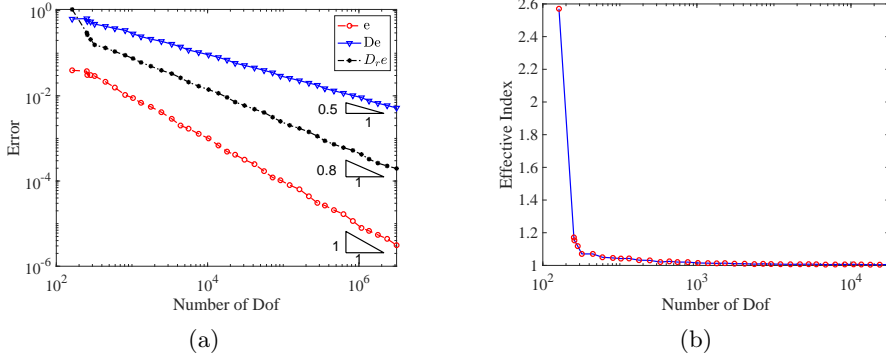


Fig. 6.4: Meshes for numerical example3: (a) Initial mesh; (b) Adaptively refined mesh.

To quantify the performance of our new recovery-based *a posteriori* error estimator for the Laplace-Beltrami problem, the effectivity index κ is used to measure the quality of an error estimator [1,5], which is defined by the ratio between the estimated error and the exact error

$$\kappa = \frac{\|u_h - \nabla u_h\|_{L^2(\Gamma)}}{|u - u_h|_{H^1(\Gamma_h; \mathcal{T}_h)}} \quad (6.1)$$

The effectivity index is plotted in Figure 6.4b . We see that κ converges asymptotically to 1 which indicates the posteriori error estimator (5.9) is asymptotically exact.

6.4. Numerical example 4. This example is taken from [19]. The surface is the zero level of the following level set function

$$\phi(x) = 400(x_1^2 x_2^2 + x_2^2 x_3^2 + x_1^2 x_3^2) - (1 - x_1^2 - x_2^2 - x_3^2)^3 - 40.$$

The discretized surface on the initial mesh is shown in Figure 6.5a. What can be clearly seen in this figure is the high curvature parts. The initial mesh fails to resolve them. In contrast, the high curvature parts are well captured by the adaptively refined mesh as plotted in Figure 6.5b.

Figure 6.6a plot errors in term of degrees of freedom. The figure shows the optimal decay of the L^2 error and discrete H^1 semi-error. In addition, we observe that the recovered gradient error superconverges at a rate of $\mathcal{O}(h^{1.6})$. In Figure 6.6b, we graph the effectivity index κ . Figure 2 reveals that the effectivity index is close to 1 after several refinements. It illustrates that the recovery-type *a posteriori* error estimator (5.9) is asymptotically exact.

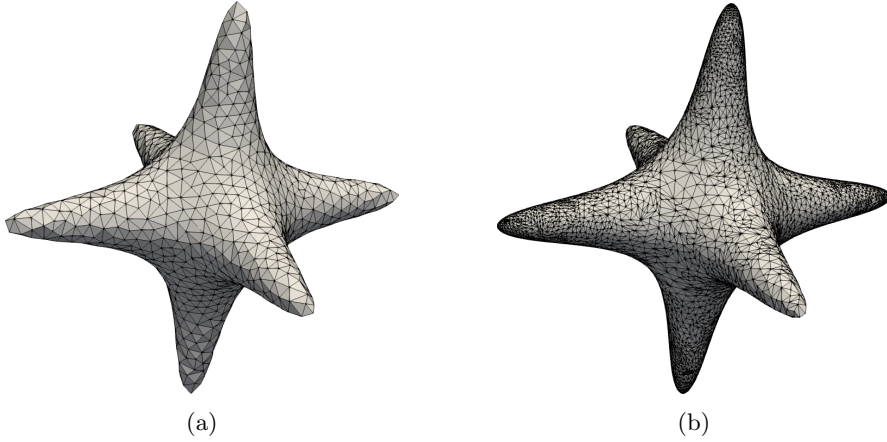


Fig. 6.5: Meshes for numerical example 4: (a) Initial mesh; (b) Adaptively refined mesh.

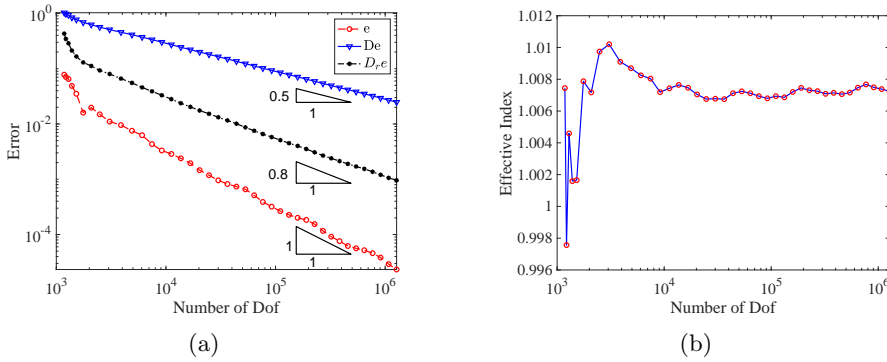


Fig. 6.6: Meshes for numerical example 4: (a) Initial mesh; (b) Adaptively refined mesh.

7. Conclusion. In this paper, we have introduced and analyzed the Crouzeix-Raviart element on a surface setting. The surface Crouzeix-Raviart element is a nonconforming element in the sense that it is only continuous at edge centers. The optimal convergence theory has also been established using a delicate argument. In addition, we have proposed a superconvergent gradient recovery for the surface Crouzeix-Raviart element. The proposed post-processing procedure is numerical proven to be able to provide a more accurate approximate gradient and asymptotically exact *a posteriori* error estimator.

Ongoing research topics include using a residue-type a posterior error estimate to conduct medius error analysis [9] and applying it to investigate surface Stokes problems and surface Navier-Stokes problems.

REFERENCES

- [1] M. AINSWORTH AND J. T. ODEN, *A posteriori error estimation in finite element analysis*, Pure and Applied Mathematics (New York), Wiley-Interscience [John Wiley & Sons], New York, 2000.
- [2] P. F. ANTONIETTI, A. DEDNER, P. MADHAVAN, S. STANGALINO, B. STINNER, AND M. VERANI, *High order discontinuous Galerkin methods for elliptic problems on surfaces*, SIAM J. Numer. Anal., 53 (2015), pp. 1145–1171.
- [3] M. ARROYO AND A. DESIMONE, *Relaxation dynamics of fluid membranes*, Phys. Rev. E, 79 (2009), p. 031915.
- [4] T. AUBIN, *Best constants in the Sobolev imbedding theorem: the Yamabe problem*, in Seminar on Differential Geometry, vol. 102 of Ann. of Math. Stud., Princeton Univ. Press, Princeton, N.J., 1982, pp. 173–184.
- [5] I. BABUŠKA AND T. STROUBOULIS, *The finite element method and its reliability*, Numerical Mathematics and Scientific Computation, The Clarendon Press, Oxford University Press, New York, 2001.
- [6] J. W. BARRETT, H. GARCKE, AND R. NÜRNBERG, *Numerical computations of the dynamics of fluidic membranes and vesicles*, Phys. Rev. E, 92 (2015), p. 052704.
- [7] J. W. BARRETT, H. GARCKE, AND R. NÜRNBERG, *A stable numerical method for the dynamics of fluidic membranes*, Numerische Mathematik, 134 (2016), pp. 783–822.
- [8] D. BRAESS, *Finite elements*, Cambridge University Press, Cambridge, third ed., 2007. Theory, fast solvers, and applications in elasticity theory, Translated from the German by Larry L. Schumaker.
- [9] S. C. BRENNER, *Forty years of the Crouzeix-Raviart element*, Numer. Methods Partial Differential Equations, 31 (2015), pp. 367–396.
- [10] S. C. BRENNER AND L. R. SCOTT, *The mathematical theory of finite element methods*, vol. 15 of Texts in Applied Mathematics, Springer, New York, third ed., 2008.
- [11] S. C. BRENNER AND L.-Y. SUNG, *Linear finite element methods for planar linear elasticity*, Math. Comp., 59 (1992), pp. 321–338.
- [12] F. BREZZI AND M. FORTIN, *Mixed and hybrid finite element methods*, vol. 15 of Springer Series in Computational Mathematics, Springer-Verlag, New York, 1991.
- [13] E. BURMAN, P. HANSBO, M. G. LARSON, K. LARSSON, AND A. MASSING, *Finite element approximation of the laplace-beltrami operator on a surface with boundary*, Numerische Mathematik, (2018).
- [14] C. CARSTENSEN AND S. BARTELS, *Each averaging technique yields reliable a posteriori error control in FEM on unstructured grids. I. Low order conforming, nonconforming, and mixed FEM*, Math. Comp., 71 (2002), pp. 945–969.
- [15] L. CHEN, *Short implementation of bisection in MATLAB*, in Recent advances in computational sciences, World Sci. Publ., Hackensack, NJ, 2008, pp. 318–332.
- [16] P. G. CIARLET, *The finite element method for elliptic problems*, vol. 40 of Classics in Applied Mathematics, Society for Industrial and Applied Mathematics (SIAM), Philadelphia, PA, 2002. Reprint of the 1978 original [North-Holland, Amsterdam; MR0520174 (58 #25001)].
- [17] B. COCKBURN AND A. DEMLOW, *Hybridizable discontinuous Galerkin and mixed finite element methods for elliptic problems on surfaces*, Math. Comp., 85 (2016), pp. 2609–2638.
- [18] M. CROUZEIX AND P.-A. RAVIART, *Conforming and nonconforming finite element methods for solving the stationary Stokes equations. I*, Rev. Française Automat. Informat. Recherche Opérationnelle Sér. Rouge, 7 (1973), pp. 33–75.
- [19] A. DEDNER AND P. MADHAVAN, *Adaptive discontinuous Galerkin methods on surfaces*, Numer. Math., 132 (2016), pp. 369–398.
- [20] A. DEDNER, P. MADHAVAN, AND B. STINNER, *Analysis of the discontinuous Galerkin method for elliptic problems on surfaces*, IMA J. Numer. Anal., 33 (2013), pp. 952–973.
- [21] A. DEMLOW, *Higher-order finite element methods and pointwise error estimates for elliptic problems on surfaces*, SIAM J. Numer. Anal., 47 (2009), pp. 805–827.
- [22] A. DEMLOW AND G. DZIUK, *An adaptive finite element method for the Laplace-Beltrami operator on implicitly defined surfaces*, SIAM J. Numer. Anal., 45 (2007), pp. 421–442 (electronic).
- [23] M. P. DO CARMO, *Riemannian geometry*, Mathematics: Theory & Applications, Birkhäuser Boston, Inc., Boston, MA, 1992. Translated from the second Portuguese edition by Francis Flaherty.
- [24] G. DONG AND H. GUO, *Parametric polynomial preserving recovery on manifolds*, arXiv:1703.06509 [math.NA], 2017.
- [25] G. DZIUK, *Finite elements for the Beltrami operator on arbitrary surfaces*, in Partial differential equations and calculus of variations, vol. 1357 of Lecture Notes in Math., Springer, Berlin, 1988, pp. 142–155.

- [26] G. DZIUK AND C. M. ELLIOTT, *Finite element methods for surface PDEs*, Acta Numer., 22 (2013), pp. 289–396.
- [27] S. ELCOTT, Y. TONG, E. KANSO, P. SCHRÖDER, AND M. DESBRUN, *Stable, circulation-preserving, simplicial fluids*, ACM Trans. Graph., 26 (2007).
- [28] T.-P. FRIES, *Higher-order surface fem for incompressible navier-stokes flows on manifolds*, International Journal for Numerical Methods in Fluids, 88 (2018), pp. 55–78.
- [29] J. GRANDE AND A. REUSKEN, *A higher order finite element method for partial differential equations on surfaces*, SIAM J. Numer. Anal., 54 (2016), pp. 388–414.
- [30] H. GUO AND Z. ZHANG, *Gradient recovery for the Crouzeix-Raviart element*, J. Sci. Comput., 64 (2015), pp. 456–476.
- [31] K. LARSSON AND M. G. LARSON, *A continuous/discontinuous Galerkin method and a priori error estimates for the biharmonic problem on surfaces*, Math. Comp., 86 (2017), pp. 2613–2649.
- [32] J. M. LEE, *Riemannian manifolds*, vol. 176 of Graduate Texts in Mathematics, Springer-Verlag, New York, 1997. An introduction to curvature.
- [33] P. MULLEN, K. CRANE, D. PAVLOV, Y. TONG, AND M. DESBRUN, *Energy-preserving integrators for fluid animation*, ACM Trans. Graph., 28 (2009), pp. 38:1–38:8.
- [34] M. A. OLSHANSKII, A. QUAINI, REUSKEN A., AND V. YUSHUTIN, *A finite element method for the surface stokes problem*, arXiv:1801.06589 [math.NA], 2018.
- [35] M. A. OLSHANSKII, A. REUSKEN, AND J. GRANDE, *A finite element method for elliptic equations on surfaces*, SIAM J. Numer. Anal., 47 (2009), pp. 3339–3358.
- [36] M. A. OLSHANSKII AND D. SAFIN, *A narrow-band unfitted finite element method for elliptic PDEs posed on surfaces*, Math. Comp., 85 (2016), pp. 1549–1570.
- [37] K. PADBERG-GEHLE, S. REUTHER, S. PRAETORIUS, AND A. VOIGT, *Transfer operator-based extraction of coherent features on surfaces*, in Topological Methods in Data Analysis and Visualization IV, H. Carr, C. Garth, and T. Weinkauff, eds., Cham, 2017, Springer International Publishing, pp. 283–297.
- [38] A. REUSKEN, *Stream function formulation of surface stokes equations*, IMA Journal of Numerical Analysis, (2018), p. dry062.
- [39] S. REUTHER AND A. VOIGT, *Solving the incompressible surface navier-stokes equation by surface finite elements*, Physics of Fluids, 30 (2018), p. 012107.
- [40] L. RINEAU AND M. YVINEC, *3D surface mesh generation*, in CGAL User and Reference Manual, CGAL Editorial Board, 4.9 ed., 2016.
- [41] E. SASAKI, S. TAKEHIRO, AND M. YAMADA, *Bifurcation structure of two-dimensional viscous zonal flows on a rotating sphere*, Journal of Fluid Mechanics, 774 (2015), p. 224244.
- [42] H. WEI, L. CHEN, AND Y. HUANG, *Superconvergence and gradient recovery of linear finite elements for the Laplace-Beltrami operator on general surfaces*, SIAM J. Numer. Anal., 48 (2010), pp. 1920–1943.
- [43] J. WLOKA, *Partial differential equations*, Cambridge University Press, Cambridge, 1987. Translated from the German by C. B. Thomas and M. J. Thomas.
- [44] Z. ZHANG AND A. NAGA, *A new finite element gradient recovery method: superconvergence property*, SIAM J. Sci. Comput., 26 (2005), pp. 1192–1213 (electronic).